Monte Carlo simulations reveal the straightening of an end-grafted flexible chain with a rigid side chain

Marcel Hellmann,[1,2] Matthias Weiss,[2] and Dieter W. Heermann[1]
[1]*Institut für Theoretische Physik, Philosophenweg 19, Universität Heidelberg, D-69120 Heidelberg, Germany*
[2]*Cellular Biophysics Group, German Cancer Research Center, Im Neuenheimer Feld 580, D-69120 Heidelberg, Germany*
(Received 8 May 2007; published 14 August 2007)

We have studied the conformational properties of a flexible end-grafted chain (length N) with a rigid side chain (length S) by means of Monte Carlo simulations. Depending on the lengths N and S and the branching site b, we observe a considerable straightening of the flexible backbone as quantified via the gyration tensor. For $b=N$, i.e., when attaching the side chain to the free end of the flexible backbone, the effect was strongest.

DOI: 10.1103/PhysRevE.76.021802 PACS number(s): 36.20.Ey, 68.47.Pe, 68.47.Mn

I. INTRODUCTION

Polymers anchored on a locally flat substrate are of great importance for functionalized surfaces in the material sciences [1] and in biology [2]. A particular example for the latter is the protective extracellular matrix of living cells that is composed of the flexible polymer hyaluronic acid (HA) to which semiflexible aggrecan chains are attached via linker proteins [3,4]. The HA-aggrecan has recently received increased attention as it is not only used to equip cells with a protective layer but also plays an important role as a gliding surface in the articular cartilage of synovial joints [4]. Understanding the material properties of the HA-aggrecan system on the nano- and mesoscale are thus of key importance when aiming at constructing biomimetic surfaces that mimic the function of natural cartilages. In fact, on the single-molecule scale the HA-aggrecan system can be simplified to a flexible polymer attached to a planar substrate, with rigid side chains.

Flexible, self-avoiding end-grafted polymers without side chains have been studied extensively by theory, experiment, and computational approaches [5,6]. Typically, a large set of end-grafted polymers has been considered, where the grafting density σ, i.e., the distance between individual chains, was varied ("polymer brush"). In the limit of very low σ, the polymer chains can be considered as isolated entities, each acquiring approximately a half-spherical shape ("mushroom") with a radius comparable to the Flory radius $R_F=aN^{3/5}$ of a coil in a good solvent [7]. Here, a and N denote the size of a monomer and the number of monomers, respectively. In fact, a more detailed description of the polymer shape requires the gyration tensor [8,9]:

$$S_{mn}=\frac{1}{N}\sum_{i=1}^{N} r_m^{(i)} r_n^{(i)}, \tag{1}$$

where $\mathbf{r}^{(i)}$ is the position of the ith monomer with respect to the center of mass of the polymer and indices m and n denote its individual components. Using an orthogonal transformation, $\mathbf{S}$ can be converted to diagonal form with entries $L_1^2 \leqslant L_2^2 \leqslant L_3^2$ denoting the squared lengths of the principal axes of gyration while the trace of $\mathbf{S}$ yields the squared radius of gyration. The associated eigenvectors of the gyration ellipsoid are denoted by $\mathbf{v}_1$, $\mathbf{v}_2$, and $\mathbf{v}_3$, respectively.

The ratios of the principle axes of inertia quantify the deviation of the polymer shape from a sphere. Using Monte Carlo simulations it was shown that simple random walks (RW) reveal a pronounced asphericity ("asphericity of the RW") mirrored in the asymptotic ratios $\langle L_1^2\rangle:\langle L_2^2\rangle:\langle L_3^2\rangle \to 1:2.7:12.0$ [8,11]. Self-avoiding walks (SAW) show an even more aspheric shape (1:2.98:14.0) [10,11] that becomes more pronounced when attaching the SAW with one end to a flat, solid substrate (1:3.0:14.9 for $N\to\infty$) [12].

The conformational properties of polymer systems comprising side chains branching out from a flexible or semiflexible backbone at varying density ("comb polymers") have also been considered extensively in theory and simulation studies [13]. The flexibility of the entire complex has been shown to be strongly influenced by the density of flexible side chains σ_ℓ with three scaling regimes in the case for a free (i.e., not end-grafted) backbone [14,15]. One of the main results was that attaching a large number of flexible side chains stiffens an otherwise flexible backbone. Rigid side chains induced larger local fluctuations of the backbone as compared to flexible side chains [16], yet the persistence length of the entire complex was shown to grow superlinear with the length of the side chains in contrast to the much weaker dependency in the case of flexible side chains. In other words, attaching a large number of rigid side chains yields an efficient way to stiffen a flexible backbone.

Here, we investigate the conformation of a flexible, end-grafted self-avoiding chain of length N with a *single* rigid side chain (length S) by means of Monte Carlo simulations [17]. We find that attaching the side chain leads to a considerable anisotropic swelling of the flexible backbone and a straightening to a more brushlike configuration. This phenomenon does not only depend on N and S, but also on the position b at which the side chain is attached. In particular, we show that for fixed N and b the squared radius of gyration R_g^2 rises sigmoidally from the unperturbed value R_0^2 with increasing S and levels off to a constant for $S \gg b/2$. In fact, the side-chain dependent swelling of the backbone follows a scaling relation with maximum value $\Delta \sim R_0^2 b^3/N^2$. Contrary to an undisturbed end-grafted chain, the ratio R_{end}^2/R_g^2 increases with S, thus highlighting the successive breaking of isotropy that is also mirrored in dramatic changes of the ratios of the principle axes of gyration. Furthermore, for

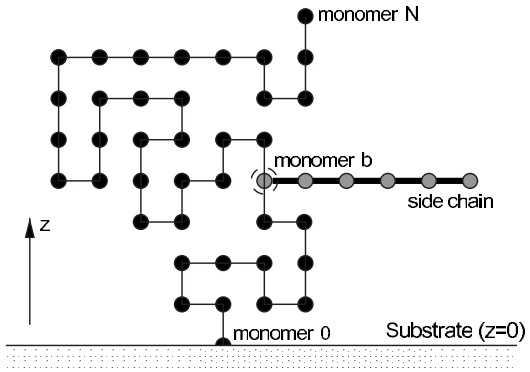

FIG. 1. Two-dimensional sketch of the self-avoiding polymer on a lattice as described in the main text. A rigid side chain (gray) is attached to the fully flexible end-grafted backbone at monomer b ("branching site"). The substrate is impenetrable, i.e., the chain conformations are restricted to the half-space $z>0$. Note that a chain of length N consists of $N+1$ monomers.

$b \approx N$ and $S \gg b/2$, the distribution of normalized angles φ ($\langle\varphi\rangle=1$) between the surface normal of the impenetrable substrate (cf. Fig. 1) and the longest axis of the backbone's gyration ellipsoid follows a Weibull distribution for all combinations N, b, and S.

II. SIMULATION METHOD

To simulate a flexible end-grafted polymer chain of length N (i.e., having $N+1$ monomers), we utilize a simple cubic lattice with unity lattice spacing (which we have taken as our unit of length). Each monomer occupies a single lattice site and self-avoidance is guaranteed by prohibiting multiple occupations. The polymer is considered in a good athermal solvent, i.e., no interactions between the monomers besides the self-avoidance are taken into account. The monomer with index 0 is placed in the plane $z=0$, and the half-space $z<0$ is chosen as impenetrable while the lattice is taken large enough to avoid influences of any other boundary. A rigid side chain of length S is attached at monomer b of the flexible chain (counted from the grafted end). Figure 1 shows a two-dimensional sketch of the model.

The flexible chain is simulated using a Verdier-Stockmayer-type algorithm allowing for kink and 90°/180°-crank shaft moves (see, e.g., Ref. [18]). Due to its rigidity, the only possible moves of the side chain are rotations by ±90° and 180° in the xy, yz, or xz plane, respectively, around the branching site b. A side chain rotation can be induced by a regular move (kink, crank) involving monomer b or randomly without translocating monomer b, i.e., by introducing a new type of move. In every attempt only those moves are accepted that lead to self-avoiding conformations while respecting the impenetrability of the substrate. Yet, "during" a rotation process of the side chain the self-avoidance can be violated. Due to the nonergodicity of all local N-conserving algorithms for SAWs [19], trapped conformations may occur that cannot be disentangled by the used algorithm. To avoid an overrepresentation of trapped conformations, the simulation is continued with a newly generated random conformation when the system appears to have run into a dead end. In practice, it turned out that only ~ 10 out of 5×10^5 configurations for $N=20$ were trapped while larger systems did not show any trapped configurations. We attribute this observation to the larger phase space of a longer polymer chain, i.e., the extremely rare trapped conformations are not encountered.

III. RESULTS AND DISCUSSION

To investigate the behavior of the described polymer system, we vary the lengths of the flexible backbone (N) and the rigid side chain (S) as well as the branching site b at which the side chain is attached to the backbone. As basic readouts, we then monitor the squared radius of gyration R_g^2, the principle moments of gyration, and the angle ϕ between the longest axis of the gyration ellipsoid and the surface normal, defined by $\cos\phi=\mathbf{v}_3\cdot\mathbf{e}_z/L_3$ [cf. Eq. (1)]. All these quantities are calculated from the backbone monomers only, in order to study the conformational differences of an end-grafted polymer with an attached side chain to one without.

We first determine the squared radius of gyration R_0^2 and the orientation angle ϕ of the gyration ellipsoid for an end-grafted flexible backbone ($N=20,\ldots,200$) *without* side chain. In agreement with Ref. [12], we observe an increase $R_0^2 \sim N^{2\nu}$ with $\nu \approx 0.59$ while the end-to-end distance is given by $R_{\mathrm{end}}^2 \approx 7.6 R_0^2$ [Fig. 2(a)]. In contrast, the average angle of orientation $\langle\phi\rangle$ only depends very weakly on N and tends linearly (i.e., without a plateau) towards an asymptotic value $\langle\phi\rangle=55°$ [Fig. 2(b), inset]. The entire probability density function $p(\phi)$ of the orientation angles for $N=20$ and 200 is shown in Fig. 2(b). Clearly, in both cases the mean $\langle\phi\rangle$ does not coincide with the plateau of the most probable value of ϕ near 90°, i.e., the gyration ellipsoid is most likely oriented parallel to the substrate ("mushroom"). It is noteworthy that the plateaulike behavior of $p(\phi)$ only emerges properly for large N, while a too short polymer shows a slight decrease of $p(\phi)$ for $\phi \to 90°$.

When attaching a rigid side chain of length S at position b to the flexible backbone (length N), we observe an increase in the radius of gyration that depends on S, b, and N. A representative example ($N=100$) is shown in Fig. 3(a). The squared radius of gyration increases sigmoidally from the unperturbed value R_0^2 with increasing S whereas the limiting plateau strongly depends on b. The gross shape of the curves can be rationalized by considering the limiting cases: for $S \to 0$ and $b \to 0$ the unperturbed backbone has to be recovered as the side chain vanishes or appears to be "glued" to the substrate surface, respectively. For large S any further increase of the side chain is not "felt" by the mushroomlike backbone, i.e., the curve should level off to a constant. In fact, we are able to collapse all data for the side-chain induced difference $\Delta=R_g^2-R_0^2$ to a single master curve [Fig. 3(b)] for various combinations of N and b by the empirical scaling:

$$x=\frac{S}{b}, \quad y=\frac{R_g^2-R_0^2}{R_0^2}\frac{N^2}{b^3}. \tag{2}$$

As a result of Eq. (2), we clearly observe that $\Delta \sim R_0^2 b^3/N^2$ in the plateau region. Thus for $b=N$ (side chain attached to the

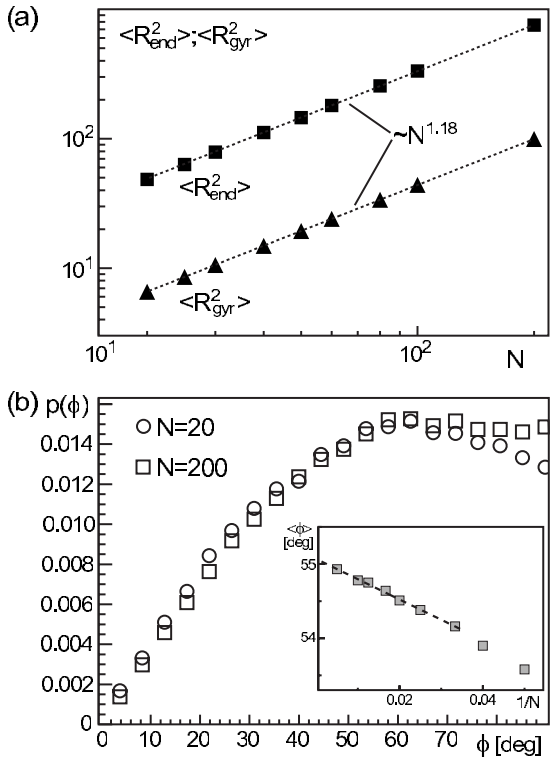

FIG. 2. (a) The radius of gyration and the end-to-end distance increase like $R_0^2 \sim N^{2\nu}$ ($\nu \approx 0.59$) for a flexible end-grafted chain (without side chain). (b) The probability density function $p(\phi)$ of the orientation angle of the polymer's gyration ellipsoid shows a plateaulike behavior for $\phi \to 90°$ in the limit of large N. Inset: The average angle $\langle \phi \rangle$, i.e., the first moment of $p(\phi)$, depends only weakly on N with an asymptotic value $\langle \phi \rangle = 55°$.

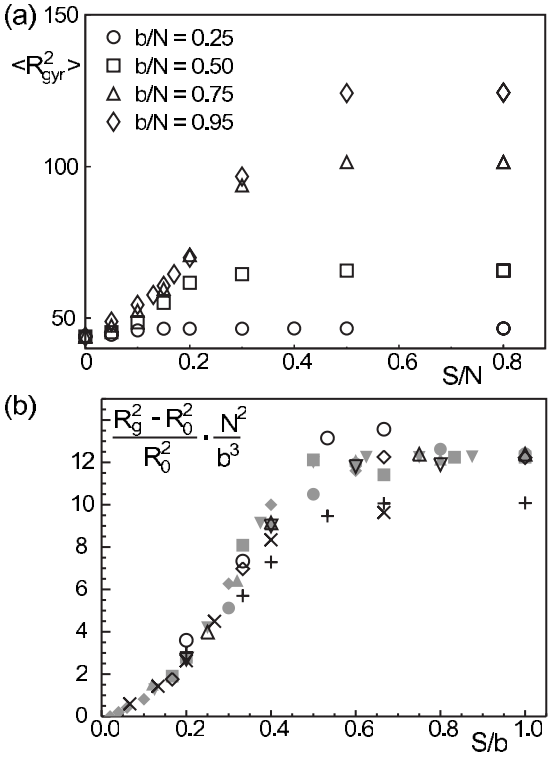

FIG. 3. (a) The squared radius of gyration $\langle R_g^2 \rangle$ increases sigmoidally with the length of the side chain S/N and levels off at increasing values with increasing b (here $N=100$). (b) All curves collapse to a single master curve when applying the scaling Eq. (2). Open black symbols: $b/N=0.25$, $N=20$, 60, 80, 100, and 120; filled gray symbols: $b/N=0.5$, $N=20$, 50, 80, 100, and 120; and crosses: $b/N=0.75$, $N=20$ and 100.

free end) the gain in length follows approximately $\Delta \sim N^2$ which is reminiscent of the behavior of flexible end-grafted chains in the "regime of stretched chains" observed in polymer brushes [7].

In Fig. 4, we have plotted the ratio between the mean squared end-to-end distance and the mean squared radius of gyration, $\theta = \langle R_{\mathrm{end}}^2 \rangle / \langle R_g^2 \rangle$, as a function of S. For a simple, free self-avoiding walk this ratio can be calculated to be $\theta = 6$ in the limit $N \to \infty$ while $\theta \approx 7.6$ for a chain attached to a solid substrate (see offset in Fig. 4 for $S=0$). Attaching a side chain results in a further increase of θ, indicating that $\langle R_{\mathrm{end}}^2 \rangle$ grows faster than $\langle R_g^2 \rangle$. Again, the effect is strongest for large values of S and b. This observation yields further evidence that the side chain, due to imposing an excluded-volume constraint, causes the flexible backbone to swell and disentangle to a more straight conformation. This picture is confirmed and refined by the subsequent results obtained from the study of the gyration tensor.

While $\langle R_g^2 \rangle$ measures the spherical size of a polymer, its actual shape is better described by the dimensions of the gyration ellipsoid L_1, L_2, and L_3. The ratio $\langle L_1^2 \rangle : \langle L_2^2 \rangle : \langle L_3^2 \rangle$ resembles the asphericity of the polymer. Our results show that for growing S $\langle L_3^2 \rangle : \langle L_1^2 \rangle$ increases up to a plateau at $S \approx 0.5N$ that depends on b — analogous to $\langle R_g^2 \rangle$. For $N=100$ and $b=0.5N$ we obtain a maximum ratio of approximately 26:1, indicating a dramatically altered conformation in comparison to a simple end-grafted chain, where 14.9:1 is found [12]. The ratio is even higher for larger values of b, that is, the backbone takes on a pronounced rodlike shape due to the attached rigid side chain.

The ratio $\langle L_2^2 \rangle : \langle L_1^2 \rangle$ between the two shorter axes of gyration shows a different behavior: For $b < 0.5N$ it changes only marginally with increasing S and takes on a value of about 3.1:1 independent of b. In contrast, for $b=0.5N$ a small but

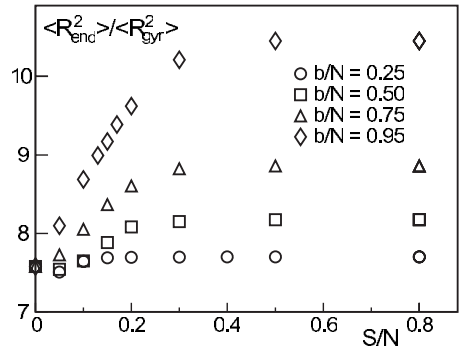

FIG. 4. The ratio $\theta = \langle R_{\mathrm{end}}^2 \rangle / \langle R_g^2 \rangle$ of the squared end-to-end distance and radius of gyration of the backbone increases with increasing length of the rigid side chain S/N (here $N=100$).

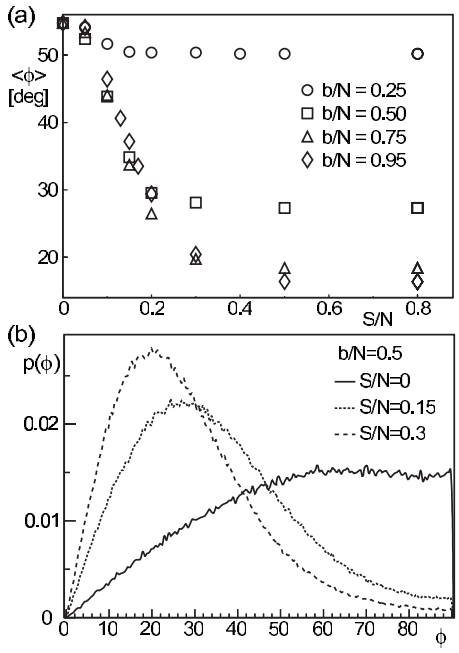

FIG. 5. (a) The average angle $\langle\phi\rangle$ between the longest axis of gyration and the substrate normal decreases for increasing lengths of the side chain S/N, indicating a straightening of the backbone. Moving the branching site b towards the free end of the backbone strongly enhances this straightening. (b) The entire distribution $p(\phi)$ shifts and becomes more narrow as S/N is decreased (here $N=100$).

appreciable increase occurs leading to a saturation value of 4:1 for $N=100$.

To confirm our results and insights derived on the basis of the gyration ellipsoid, we consider as complementary quantities the average abundance $n(90°)$ and $n(180°)$ of angles between neighboring links. Indeed, the ratio $n(90°):n(180°)$ is a good measure for the persistence of a chain as a straightening increases $n(180°)$, while a direct calculation of the backbone's persistence length suffers from the rather low numbers of monomers in the backbone. For an unperturbed chain, we have four possibilities to find an angle of 90° and one for 180°, i.e., $n(90°):n(180°)$ can be at best 4:1. Due to the self-avoidance, however, the ratio is 3.45:1 (as determined from an unperturbed chain with $N=100$). Attaching the rigid side chain at position b, we find for $N=101$, $b=50$, and $S/b=0.4$ (i.e., not yet in the saturation regime of Fig. 3) a ratio $n(90°):n(180°)=3.1:1$ for the monomers below b. In other words, below the branching point b an angle of 180° is found more often, thus confirming the straightening of the backbone. Interestingly, the persistence of the backbone above the branching point is approximately that of an unperturbed chain.

We next consider the orientation of the backbone in terms of the distribution of orientation angles $p(\phi)$ between the longest principle axis of gyration $\mathbf{v}_3$ and the surface normal. As can be seen in Fig. 5(a) for the representative example $N=100$, elongating the side chain leads to a considerable decrease of the average angle $\langle\phi\rangle$, indicating a more brushlike configuration of the backbone. This straightening becomes more pronounced when the branching site b is moved towards the free end of the backbone, i.e., for large S and $b\to N$ the backbone deviates from the surface normal by less than 20°. Concomitant to the decrease of the average orientation angle, the entire distribution $p(\phi)$ changes and assumes a more compact, i.e., narrow shape around the mean $\langle\phi\rangle$ for large S [Fig. 5(b)]. The decrease in width of the distribution accompanying the decrease of the average highlights the brushlike conformation of the backbone.

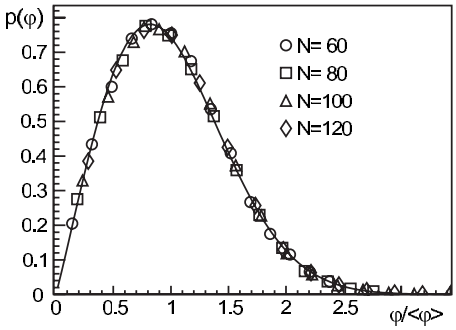

FIG. 6. Normalizing the average angle, i.e., setting $\varphi=\phi/\langle\phi\rangle$, for $b\approx N$ leads to a collapse of all distributions $p(\varphi)$ for various N,S with $S/N=0.3$ (symbols). The curve is best described by Eq. (3) (full line).

Indeed, the compact shape of $p(\phi)$ is a generic feature of the backbone for $b\to N$ and large S. This is reflected by the fact that all distributions can be collapsed to a single master curve

$$p(\varphi)=\frac{k\varphi^{k-1}}{\lambda^k}\exp\left\{-\left(\frac{\varphi}{\lambda}\right)^k\right\} \tag{3}$$

with $k\approx 2$, $\lambda\approx 1$, when considering the normalized angle $\varphi=\phi/\langle\phi\rangle$ and fixing $b/N=$const and $S/N=$const (Fig. 6).

IV. CONCLUSIONS

We conducted Monte Carlo simulations using a flexible polymer backbone, end-grafted to a solid substrate, with a rigid side chain attached to it. From the behavior of the backbone's radius of gyration and the length and orientation of its longest principle axis of gyration, we are able to conclude that attaching a rigid side chain leads to a straightening of the backbone to a more brushlike configuration. Depending on the side chain length S and the branching site b, the radius of gyration and the gyration component perpendicular to the substrate is enhanced while the average orientation tends towards the surface normal. The effects of the side chain are strongest in the case of large b and S.

For an undisturbed end-grafted chain [Fig. 2(b)] the probability density $p(\phi)$ shows a plateau for angles near to 90°, resembling a coiled conformation (mushroom). Attaching a stiff side chain leads to a shift to smaller angles and a narrowing of $p(\phi)$ [Fig. 5(b)]. It is found that $p(\phi)$ can be scaled using a Weibull distribution [Eq. (3)]. According to the changes of $p(\phi)$ the arithmetic mean $\langle\phi\rangle$ changes starting at about 55° in the case of an undisturbed chain to smaller

values when a side chain is attached [Fig. 5(a)].

The behavior of the radius of gyration as well as of the ratio $\langle R_{\mathrm{end}}^2\rangle/\langle R_g^2\rangle$ indicates a swelling and straightening of the backbone due to the presence of the stiff side chain. The backbone's change from a mushroom to a more rodlike conformation is also reflected in the ratios between the axes of gyration: While the two smaller principal axes only show minor changes, the longest principal axis is increased manifold, e.g., 26-fold for $b/N=1/2$. Furthermore, the increase in the radius of gyration follows an empirical scaling with maximum value b^3/N^2 which implicates a more brushlike growth of R_g^2 with the backbone length N.

It will be interesting to examine the influence of semiflexibility of the side chain to obtain a more realistic representation of the above described HA-aggrecan system. To approach the biological setting, e.g., the protective extracellular matrix, the phase diagram of end-grafted polymers with an attached side chain at varying surface densities will be of great interest. Work along these lines is currently underway.

ACKNOWLEDGMENTS

We would like to thank Dennis Große for providing the initial code and Manfred Bohn for helpful discussions. This work was supported by the Institute for Modeling and Simulation in the Biosciences (BIOMS) in Heidelberg.

[1] B. Zhao and W. Brittain, Prog. Polym. Sci. **25**, 677 (2000).
[2] E. Sackmann and M. Tanaka, Trends Biotechnol. **18**, 58 (2000).
[3] G. Lee, B. Johnstone, K. Jacobson, and B. Caterson, J. Cell Biol. **123**, 1899 (1993).
[4] C. Kiani, L. Chen, Y. Wu, A. Yee, and B. Yang, Cell Res. **12**, 19 (2002).
[5] S. Milner, Science **251**, 905 (1991).
[6] A. Halperin, M. Tirrell, and T. Lodge, Adv. Polym. Sci. **100**, 31 (1991).
[7] P. G. de Gennes, Macromolecules **13**, 1069 (1980).
[8] K. Šolc and W. H. Stockmayer, J. Chem. Phys. **54**, 2756 (1971).
[9] K. Šolc, J. Chem. Phys. **55**, 335 (1971).
[10] D. M. Ceperly, M. H. Kalos, and J. L. Lebowitz, Macromolecules **14**, 1472 (1981).
[11] W. Bruns, Makromol. Chem., Theory Simul. **1**, 287 (1992).
[12] J. Huang, W. Jiang, and S. Han, Macromol. Theory Simul. **10**, 339 (2001).
[13] J. J. Freire, Adv. Polym. Sci. **143**, 35 (1999).
[14] G. H. Fredrickson, Macromolecules **26**, 2825 (1993).
[15] Y. Rouault and O. Borisov, Macromolecules **29**, 2605 (1996).
[16] M. Saariaho, A. Subbotin, I. Szleifer, O. Ikkala, and G. ten Brinke, Macromolecules **32**, 4439 (1999).
[17] K. Binder and D. W. Heermann, *Monte Carlo Simulation in Statistical Physics: An Introduction* (Springer-Verlag, Berlin, 2002).
[18] *Monte Carlo and Molecular Dynamics Simulations in Polymer Science*, edited by K. Binder (Oxford University Press, New York, 1995).
[19] N. Madras and A. D. Sokal, J. Stat. Phys. **47**, 573 (1987).